Proceedings of 2005 CACS Automatic Control Conference
Tainan, Taiwan, Nov 18-19, 2005

Kinematics Control of an Omnidirectional Mobile Robot

Ching-Chih Tsai*, Li-Bin Jiang, Tai-Yu Wang, Tung-Sheng Wang
Deaprtment of Electrical Engineering, National Chung Hsing University
250,Kuo Kuang Road,Taichung 402, Taiwan
*Tel: (04) 22851549,*Fax: (04) 22851410
***E-mail: cctsai@dragon.nchu.edu.tw**

摘要

本文的目的是推導出全方位輪式行動機器人之運動學模型，並提出此機器人之非線性運動學控制方法。基於回授線性化之運動學控制器被提出來達到點對點(調整)與軌跡追蹤控制。模擬與實驗結果指出所提出之控制方法的可行性與有效性。
關鍵詞：回授線性化、運動學模型、行動機器人、全方位、調整、軌跡追蹤。

Abstract

This paper presents methodologies for kinematic modeling and nonlinear control of an omnidirectional wheeled mobile robot (see Figure 1). Kinematic model of the robot is derived as well. A kinematics controller is proposed based on feedback linearization to achieve point stabilization and trajectory tracking. Simulations and experimental results are conducted to show the feasibility and efficacy of the proposed control methods.
Keywords : Feedback linearization, kinematic model, mobile robot, omnidirectional, point stabilization, trajectory tracking.

1. Introduction

In recent years, the mobile robot has become increasingly important and extensively useful in the human daily life. Among several kinds of mobile robots, omnidirectional mobile robots have even attracted much attention in the world cup soccer robots competition in the Robo-Cup association. Unlike conventional two-wheeled or four-wheeled car-like mobile robots, the omnidirectional mobile mechanism has the agile ability to move toward any direction and to simultaneously attain any desired orientation. Moreover, the maneuvering capability is particularly useful in designing advanced home-care and nursing-care mobile vehicles or manipulators.

Omnidirectional mobile robots have been investigated by several researchers. Pin *et al.* [1] presented the concepts for a family of holonomic wheeled platforms that feature full omnidirectionality with simultaneous and independent controlled and translational capabilities. Jung *et al.* [2] constructed a kind of omnidirectional base, derived its kinematical and dynamic models, and then presented a fuzzy controller to steer the robot. Kalmár-Nagy *et al.* [3] in Cornell University proposed an innovative method of generating near-optimal trajectories for an omnidirectional robot; this method provided an efficient method of path planning and allowed a large number of possible scenarios to be explored in real time. William II *et al.* [4] presented a dynamic model for omnidirectional wheeled mobile robots, considering the occurrence of slip between the wheels and motion surface.

The objective of this paper is to put emphasis on applying nonlinear control theory to construct two kinematics PI controllers for the omnidirectional mobile robot. The paper has two principal contributions; one is that the controllers are proven globally asymptotical stability; and the other is that both computer simulations and experimental results are performed on a laboratory-based omnidirectional mobile base with three independent driving wheels equally spaced at 120 degrees. The proposed control methods assume that the position and orientation of the mobile base can be directly measured. Moreover, the developed techniques are particularly useful in developing home-care or nursing-care omnidirectional mobile manipulators.

The rest of this paper is organized as follows. Section 2 describes the physical structure of the omnidirectional mobile base. Section 3 develops the kinematics model of the omnidirectional mobile base. Section 4 elucidates how to design kinematics PI controller via feedback linearization to achieve point stabilization and trajectory tracking. Section 5 conducts several simulations that are used for illustration of the effectiveness of the proposed control methods. Section 6 presents experiment results of the purposed control law. Section 7 states the concluding remarks of the paper.

2. Brief Description of the Experimental Omnidirectional Mobile Robot

The purposed omnidirectional mobile robot in the section is composed of three omnidirectional wheels manufactured by the Kornylak Corporation. Fig. 1 displays the omnidirectional mobile mechanism. The special feature of the omnidirectional mobile robot hinges on the wheels that allow free motions in any direction that is not parallel to the wheel's driving direction. Fig. 2 shows the structure and all the possible movement directions of one omnidirectional wheel. By combining three wheels, we know that each wheel is able to apply a force on the center of mass of the omnidirectional vehicle and each wheel has some axis along which it can freely rotate. Thus, we will obtain a velocity induced by other two wheels in this direction. Hence, via the suitable structure design, this kind of the mobile robot base can make the robot

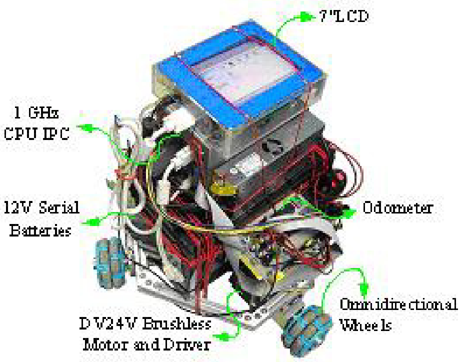

Fig. 1. Photograph of the mobile base.

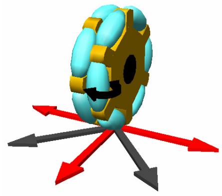

Fig. 2. The omni-directional wheels.

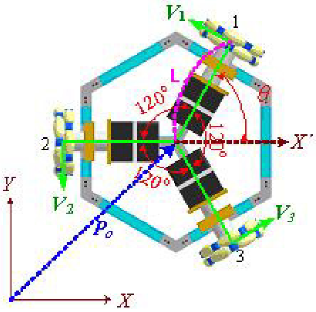

Fig. 3. Geometry of the omnidirectional robot.

move any direction, and hence construct omnidirectional maneuvering capability.

3. Kinematics Model

This section aims to describe the kinematic model of this kind of robot. Fig.3 depicts its kinematic diagram that is used to find the kinematic model of the robot, where θ denotes the vehicle orientation. Before doing so, one considers the following rotation matrix

$$R(\theta)=\begin{bmatrix}\cos\theta & -\sin\theta\\ \sin\theta & \cos\theta\end{bmatrix} \tag{1}$$

where θ is the rotation angle which is positive in the counterclockwise direction. As can be seen in Fig.3, P_0 denotes the position of the center of mass with respect to the world frame, i.e., $P_0=\begin{bmatrix}x & y\end{bmatrix}^T$ .The position $\begin{bmatrix}x_i & y_i\end{bmatrix}^T$ of each wheel can be given with respect to the center of mass of the robot, i.e., for *i=1,2,3.*,

$$P_i=\begin{bmatrix}x_i\\ y_i\end{bmatrix}=R(\theta)\cdot L\begin{bmatrix}1\\0\end{bmatrix} \tag{2}$$

where the parameter L is the distance from each wheel to the center of mass. Hence, we have the following three vectors

$$P_1=R(0)\cdot L\begin{bmatrix}1\\0\end{bmatrix}=L\begin{bmatrix}1\\0\end{bmatrix},\quad P_2=R(\frac{2\pi}{3})\cdot L\begin{bmatrix}1\\0\end{bmatrix}=\frac{L}{2}\begin{bmatrix}-1\\ \sqrt{3}\end{bmatrix}$$

$$P_3=R(\frac{4\pi}{3})\cdot L\begin{bmatrix}1\\0\end{bmatrix}=-\frac{L}{2}\begin{bmatrix}1\\ \sqrt{3}\end{bmatrix}$$

The normal unit vectors D_i of each wheel, representing the translational direction, are described as follows.

$$D_i=\frac{1}{L}R(\frac{\pi}{2})P_i,\, i=1,2,3 \tag{3}$$

which yields

$$D_1=\begin{bmatrix}0\\1\end{bmatrix}\qquad D_2=-\frac{1}{2}\begin{bmatrix}\sqrt{3}\\1\end{bmatrix}\qquad D_3=\frac{1}{2}\begin{bmatrix}\sqrt{3}\\-1\end{bmatrix}$$

With the aforementioned notation, the position and velocity of each wheel with respect to the world frame are then expressed by, for *i=1,2,3*

$$r_i=P_0+R(\theta+\frac{2\pi}{3}(i-1))P_i,\quad v_i=\dot{P}_0+\dot{R}(\theta+\frac{2\pi}{3}(i-1))P_i \tag{4}$$

Then the translational velocity V_i of each wheel is obtained from

$$\begin{aligned}V_i&=v_i^T(R(\theta+\frac{2\pi}{3}(i-1))D_i)\\&=\dot{P}_0^T R(\theta+\frac{2\pi}{3}(i-1))D_i+\dot{P}_i^T\dot{R}^T(\theta+\frac{2\pi}{3}(i-1))R(\theta+\frac{2\pi}{3}(i-1))D_i\end{aligned} \tag{5}$$

Thus, one obtains

$$V_1=-\sin\theta\cdot\dot{x}+\cos\theta\cdot\dot{y}+L\dot{\theta}$$

$$V_2=-\sin(\frac{\pi}{3}-\theta)\cdot\dot{x}-\cos(\frac{\pi}{3}-\theta)\cdot\dot{y}+L\dot{\theta}$$

$$V_3=\sin(\frac{\pi}{3}+\theta)\cdot\dot{x}+\cos(\frac{\pi}{3}+\theta)\cdot\dot{y}+L\dot{\theta}$$

which can be rewritten in the vector-matrix form

$$\begin{bmatrix}V_1\\V_2\\V_3\end{bmatrix}=\begin{bmatrix}R\omega_1\\R\omega_2\\R\omega_3\end{bmatrix}=P(\theta)\begin{bmatrix}\dot{x}\\ \dot{y}\\ \dot{\theta}\end{bmatrix} \tag{6}$$

where

$$P(\theta)=\begin{bmatrix}-\sin\theta & \cos\theta & L\\ -\sin(\frac{\pi}{3}-\theta) & -\cos(\frac{\pi}{3}-\theta) & L\\ \sin(\frac{\pi}{3}+\theta) & -\cos(\frac{\pi}{3}+\theta) & L\end{bmatrix}$$

and ω_i, i=1,2,3, denotes the angular velocity of each wheel, respectively. Notice that the matrix $P(\theta)$ is always nonsigular for any θ, and

$$P^{-1}(\theta)=\begin{bmatrix}-\frac{2}{3}\sin\theta & -\frac{2}{3}\sin(\frac{\pi}{3}-\theta) & \frac{2}{3}\sin(\frac{\pi}{3}+\theta)\\ \frac{2}{3}\cos\theta & -\frac{2}{3}\cos(\frac{\pi}{3}-\theta) & -\frac{2}{3}\cos(\frac{\pi}{3}+\theta)\\ \frac{1}{3L} & \frac{1}{3L} & \frac{1}{3L}\end{bmatrix}$$

4. PI Kinematics Control

This section is devoted to designing two kinematics PI controllers to achieve point-to-point stabilization and trajectory tracking with slow motion speed (the speed is less than *1 m/sec*). In doing so, from (6), we have

$$\begin{bmatrix} \dot{x} \\ \dot{y} \\ \dot{\theta} \end{bmatrix} = P^{-1}(\theta)\begin{bmatrix} V_1 \\ V_2 \\ V_3 \end{bmatrix} \quad (12)$$

4.1 Point-to-point Stabilization

The control goal of the point-to-point stabilization is to find the controlled velocity vector $\begin{bmatrix} V_1 & V_2 & V_3 \end{bmatrix}^T$ or the controlled angular velocity vector $\begin{bmatrix} \omega_1 & \omega_2 & \omega_3 \end{bmatrix}^T$ to steer the mobile robot from the starting posture $\begin{bmatrix} x_0 & y_0 & \theta_0 \end{bmatrix}^T$ to any desired posture $\begin{bmatrix} x_d & y_d & \theta_d \end{bmatrix}^T$. Note that the current posture of the mobile base is $\begin{bmatrix} x & y & \theta \end{bmatrix}^T$. To design the controller, one defines the pose error vector. The control goal is to find the controlled velocity vector

$$\begin{bmatrix} x_e \\ y_e \\ \theta_e \end{bmatrix} = \begin{bmatrix} x \\ y \\ \theta \end{bmatrix} - \begin{bmatrix} x_d \\ y_d \\ \theta_d \end{bmatrix} \quad (13)$$

which gives

$$\begin{bmatrix} \dot{x}_e \\ \dot{y}_e \\ \dot{\theta}_e \end{bmatrix} = \begin{bmatrix} \dot{x} \\ \dot{y} \\ \dot{\theta} \end{bmatrix} = P^{-1}(\theta)\begin{bmatrix} V_1 \\ V_2 \\ V_3 \end{bmatrix} \quad (14)$$

To asymptotically stabilize the system, we propose the PI control law where the gain matrices, K_P and K_I, are symmetric and positive definite.

$$\begin{bmatrix} V_1 \\ V_2 \\ V_3 \end{bmatrix} = P(\theta)\left(-K_p \begin{bmatrix} x_e \\ y_e \\ \theta_e \end{bmatrix} - K_I \begin{bmatrix} \int x_e \\ \int y_e \\ \int \theta_e \end{bmatrix} \right), \quad K_P = K_P^T > 0, \; K_I = K_I^T > 0 \quad (15)$$

Taking (15) into (14), the closed-loop error system becomes

$$\begin{bmatrix} \dot{x}_e \\ \dot{y}_e \\ \dot{\theta}_e \end{bmatrix} = P^{-1}(\theta)P(\theta)\left(-K_p \begin{bmatrix} x_e \\ y_e \\ \theta_e \end{bmatrix} - K_I \begin{bmatrix} \int x_e \\ \int y_e \\ \int \theta_e \end{bmatrix} \right) = -K_p \begin{bmatrix} x_e \\ y_e \\ \theta_e \end{bmatrix} - K_I \begin{bmatrix} \int x_e \\ \int y_e \\ \int \theta_e \end{bmatrix}$$

For the asymptotical stability of the closed-loop error system, a radially unbounded Lyapunov function candidate is chosen as follows:

$$V = \frac{1}{2}\begin{bmatrix} x_e & y_e & \theta_e \end{bmatrix}\begin{bmatrix} x_e \\ y_e \\ \theta_e \end{bmatrix} + \frac{1}{2}\begin{bmatrix} \int x_e & \int y_e & \int \theta_e \end{bmatrix} K_I \begin{bmatrix} \int x_e \\ \int y_e \\ \int \theta_e \end{bmatrix}$$

Taking the time derivative of V along the trajectory of (14) obtains

$$\dot{V} = \begin{bmatrix} x_e & y_e & \theta_e \end{bmatrix}\begin{bmatrix} \dot{x}_e \\ \dot{y}_e \\ \dot{\theta}_e \end{bmatrix} + \begin{bmatrix} \int x_e & \int y_e & \int \theta_e \end{bmatrix} K_I \begin{bmatrix} x_e \\ y_e \\ \theta_e \end{bmatrix}$$

$$= \begin{bmatrix} x_e & y_e & \theta_e \end{bmatrix}\left(-K_p \begin{bmatrix} x_e \\ y_e \\ \theta_e \end{bmatrix} - K_I \begin{bmatrix} \int x_e \\ \int y_e \\ \int \theta_e \end{bmatrix} \right) + \begin{bmatrix} \int x_e & \int y_e & \int \theta_e \end{bmatrix} K_I \begin{bmatrix} x_e \\ y_e \\ \theta_e \end{bmatrix}$$

$$= -\begin{bmatrix} x_e & y_e & \theta_e \end{bmatrix} K_p \begin{bmatrix} x_e \\ y_e \\ \theta_e \end{bmatrix} < 0$$

Since $\dot{V}$ is negative definite, Barbalat's lemma implies that

$$\begin{bmatrix} x_e & y_e & \delta_e \end{bmatrix}^T \to 0 \quad as \quad t \to \infty .$$

Moreover, it is easily shown that the origin, $\begin{bmatrix} 0 & 0 & 0 \end{bmatrix}^T$, is globally asymptotically , that is, position and orientation errors asymptotically approach zero as time tend to infinity.

Considering the speed limitations of all the motors and ignoring the integral control action, one may obtain a more pragmatic control law

$$\begin{bmatrix} V_1 \\ V_2 \\ V_3 \end{bmatrix} = P(\theta)\left(-K_p \begin{bmatrix} sat(x_e) \\ sat(y_e) \\ sat(\theta_e) \end{bmatrix} \right) \quad (16)$$

where the saturation function $sat(\bullet)$ is given by

$$sat(y) = \begin{cases} y_{\max} & , if\; y \ge y_{\max} \\ y & , if\; y_{\min} \le y \le y_{\max} \\ y_{\min} & , if\; y \le y_{\min} \end{cases}$$

The control law (16) can be proven asymptotically stable using the similar procedure.

4.2 Trajectory Tracking Control

This subsection considers the time-varying trajectory tracking problem. Unlike all nonholonomic conventional mobile robots, the trajectories of the omnidirectional mobile base can not be generated using their kinematics model, i.e., any smooth trajectory for the omnidirectional robot can be arbitrarily planned. Given the time-varying path $\begin{bmatrix} x_d(t) & y_d(t) & \theta_d(t) \end{bmatrix}^T$, one defines the following tracking error vector.

$$\begin{bmatrix} x_e(t) \\ y_e(t) \\ \theta_e(t) \end{bmatrix} = \begin{bmatrix} x(t) \\ y(t) \\ \theta(t) \end{bmatrix} - \begin{bmatrix} x_d(t) \\ y_d(t) \\ \theta_d(t) \end{bmatrix}$$

Thus, one obtains

$$\begin{bmatrix} \dot{x}_e \\ \dot{y}_e \\ \dot{\theta}_e \end{bmatrix} = \begin{bmatrix} \dot{x} \\ \dot{y} \\ \dot{\theta} \end{bmatrix} - \begin{bmatrix} \dot{x}_d \\ \dot{y}_d \\ \dot{\theta}_d \end{bmatrix} = P^{-1}(\theta)\begin{bmatrix} V_1 \\ V_2 \\ V_3 \end{bmatrix} - \begin{bmatrix} \dot{x}_d \\ \dot{y}_d \\ \dot{\theta}_d \end{bmatrix} \quad (17)$$

Similarly, the control goal is to find a set of control velocity vector $\begin{bmatrix} V_1 & V_2 & V_3 \end{bmatrix}^T$ such that the closed loop error system is asymptotically stable. In doing so, we propose

$$\begin{bmatrix} V_1 \\ V_2 \\ V_3 \end{bmatrix} = P(\theta)\left(-K_p \begin{bmatrix} x_e \\ y_e \\ \theta_e \end{bmatrix} - K_I \begin{bmatrix} \int x_e \\ \int y_e \\ \int \theta_e \end{bmatrix} + \begin{bmatrix} \dot{x}_d \\ \dot{y}_d \\ \dot{\theta}_d \end{bmatrix} \right) \quad (18)$$

which leads to the underlying closed-loop error system

$$\begin{bmatrix} \dot{x}_e \\ \dot{y}_e \\ \dot{\theta}_e \end{bmatrix} = P^{-1}(\theta)P(\theta)\left(-K_p \begin{bmatrix} x_e \\ y_e \\ \theta_e \end{bmatrix} - K_I \begin{bmatrix} \int x_e \\ \int y_e \\ \int \theta_e \end{bmatrix} + \begin{bmatrix} \dot{x}_d \\ \dot{y}_d \\ \dot{\theta}_d \end{bmatrix} \right) - \begin{bmatrix} \dot{x}_d \\ \dot{y}_d \\ \dot{\theta}_d \end{bmatrix}$$
$$= -K_p \begin{bmatrix} x_e \\ y_e \\ \theta_e \end{bmatrix} - K_I \begin{bmatrix} \int x_e \\ \int y_e \\ \int \theta_e \end{bmatrix} + \begin{bmatrix} \dot{x}_d \\ \dot{y}_d \\ \dot{\theta}_d \end{bmatrix} - \begin{bmatrix} \dot{x}_d \\ \dot{y}_d \\ \dot{\theta}_d \end{bmatrix} = -K_p \begin{bmatrix} x_e \\ y_e \\ \theta_e \end{bmatrix} - K_I \begin{bmatrix} \int x_e \\ \int y_e \\ \int \theta_e \end{bmatrix} \quad (19)$$

The globally asymptotical stability of the closed-loop error system can be easily achieved by selecting the quadratic Lyapunov function

$$V = \frac{1}{2}\begin{bmatrix} x_e & y_e & \theta_e \end{bmatrix} \begin{bmatrix} x_e \\ y_e \\ \theta_e \end{bmatrix} + \frac{1}{2}\begin{bmatrix} \int x_e & \int y_e & \int \theta_e \end{bmatrix} K_I \begin{bmatrix} \int x_e \\ \int y_e \\ \int \theta_e \end{bmatrix}$$

5. Simulations and Discussion

The aim of the simulations is to examine the effectiveness and performance of the proposed PI control methods. Two diagonal gain matrices, K_p =diag{5,5,5}and K_i =diag{0.2,0.2,0.2}, were adopted for the proposed kinematics controllers. These simulations, programmed by Matlab 6.5, were performed with the parameter L of 23 cm.

5.1 Point-to-point Stabilization

The first simulation was conducted to investigate the point-to-point regulation performance of the proposed kinematics PI controller. The initial posture of the omnidirectional mobile base is assumed at the origin, $\begin{bmatrix} X_0 & Y_0 & \theta_0 \end{bmatrix} = \begin{bmatrix} 0 & 0 & 0 \end{bmatrix}$. The desired final 16 goal postures are located on the circle, given by

$$\begin{bmatrix} X_d & Y_d & \theta_d \end{bmatrix} = \begin{bmatrix} 10\cos(\frac{n\pi}{8}) & 10\sin(\frac{n\pi}{8}) & 1.5 \end{bmatrix}^T, n = 0,1,...,15.$$

Fig. 4 depicts all the simulated trajectories of the omnidirectional mobile base from the origin to the goal postures. These results indicate that these trajectories have minimum distances, i.e., the mobile base moves along with straight lines toward the goal posture. More importantly, the mobile base moves toward any direction and simultaneously attains the desired orientation, showing the unique property of the omnidirectional wheeled mobile robot.

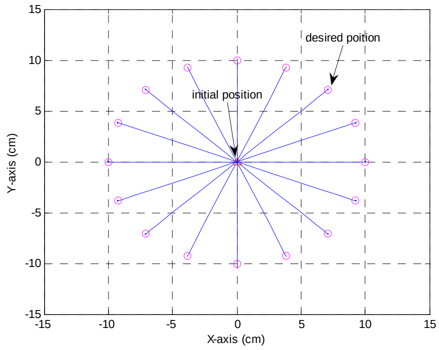

Fig. 4. Simulated trajectories of the proposed kinematics controller for achieving point-to-point stabilization.

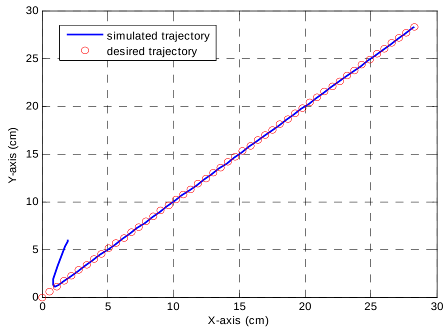

Fig. 5. Straight-line trajectories of the omnidirectional mobile base.

5.2 Straight-line Trajectory Tracking

The second simulation was used to study the trajectory tracking performance of the kinematics tracking controller. The initial posture and desired trajectory are respectively given by $(X_o, Y_o, \theta_o) = (2,\ 7,\ 0)$, and

$$\begin{pmatrix} X_d & Y_d & \theta_d \end{pmatrix} = \begin{pmatrix} X_{do} + vt\cos(\theta) & Y_{do} + vt\sin(\theta) & \frac{\pi}{4} \end{pmatrix}$$

where $X_{do} = Y_{do} = 0, \quad v = 2, \quad t \geq 0$

Fig. 5 shows the simulated straight-line trajectory of the omnidirectional mobile robot. These results indicate that the proposed controller is capable of steering the mobile base to exponentially follow the desired line path.

5.3 Circular Trajectory Tracking

This subsection aims at observing the behavior of the PI controllers while the omnidirectional mobile base is moving along a circular path. The simulation of the circular trajectory tracking was performed with the following parameters: $\omega_o = \frac{\pi}{2}$ (rad/sec), $\omega_r = 0.2$ (rad/sec), $r = 2$ (cm), $X_{do} = 0$, $Y_{do} = 0$. The starting posture is $(X_o, Y_o, \theta_o) = (0.5,\ 0.5,\ 0)$, and the desired trajectory is

$$\begin{pmatrix} X_d & Y_d & \theta_d \end{pmatrix}$$
$$= \begin{pmatrix} X_{do} + r\times\cos(\omega_o + \omega_r t) & Y_{do} + r\times\sin(\omega_o + \omega_r t) & \omega_o + \omega_r t \end{pmatrix}$$

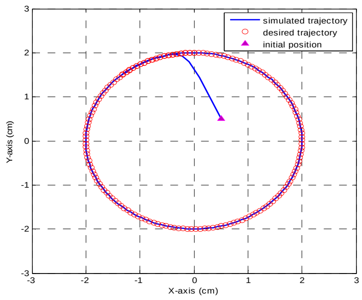

Fig. 6. Circular trajectory of the omnidirectional mobile robot .

Fig. 6 depicts the simulation result of the circular trajectory tracking for the omnidirectional mobile base. These results indicate the kinematics controller has been shown useful for achieving the circular trajectory tracking.

5.4 Elliptic Trajectory Tracking

The last simulation was utilized to explore how the PI controllers steer the robot to track an elliptic trajectory described by

$$\left(X_d \quad Y_d \quad \theta_d\right) = \left(X_{do} + r_1 \times \cos(\omega_o + \omega_r t) \quad Y_{do} + r_2 \times \sin(\omega_o + \omega_r t) \quad \omega_o + \omega_r t\right),$$

and assume that robots get started at zero initial posture, $\left(X_o,\ Y_o,\ \theta_o\right) = \left(0,\ 0,\ 0\right)$. The parameters in the elliptic trajectory tracking simulation are given as follows: $\omega_o = 1$ (rad/sec), $\omega_r = 0.2$ (rad/sec), $r_1 = 2$ (cm), $r_2 = 4$ (cm), $Y_{do} = 0$, $X_{do} = 0$.

Fig. 7 shows the elliptic trajectories of the omnidirectional mobile base. These results show that the kinematics controller is capable of steering the omnidirectional mobile base to exactly move along the elliptic trajectory.

6. Experimental Results and Discussion

The mobile robot shown in Fig.1is equipped with the following components: i) a 7” LCD monitor; ii) industrial personal computer (IPC); iii) two odometers; iv) two 12V serial batteries; v) three DC24V brushless servomotors with drivers; vi) three omnidirectional wheels. The IPC is composed of a one GHz CPU, 512 MB SDRAM, two GB CF memory card, 8255 card, and digital-to-analog card (PIO-DA9). Three driving omnidirectional wheels are driven by three DC24V brushless servomotors with three mounted encoders of delivering the signals of 300 pulses per revolution. Two diagonal gain matrices, K_p =diag{5,5,5}and K_i =diag{0.2,0.2, 0.2}, were adopted for the proposed kinematics controllers.

6.1 Point-to-point Stabilization

Fig. 8depicts the experiment results of the point-to-point regulation law. The initial posture and the final postures of the omnidirectional mobile base were set as $\left(X_o,\ Y_o,\ \theta_o\right) = \left(0,\ 0,\ 0\right)$, and

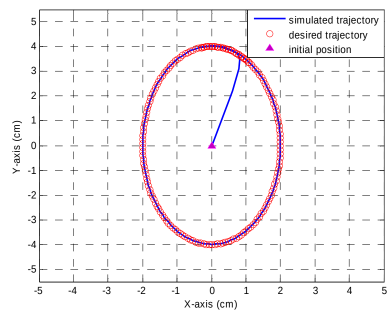

Fig. 7. Elliptic trajectory of the omnidirectional mobile base.

$\left(X_d,\ Y_d,\ \theta_d\right) = \left(100 \times \cos(\theta),\ 100 \times \sin(\theta),\ 90^\circ\right)$, $\theta = 0^\circ,\ 45^\circ,\ 90^\circ,\ 135^\circ,\ 180^\circ,\ 225^\circ,\ 270^\circ,\ 315^\circ$, respectively. The experiment results show that the mobile base with the proposed PI control method is capable of reaching the desired posture with satisfactory performance.

6.2 Straight-Line Trajectory Tracking

Fig. 9 presents the experiment result of the straight-line trajectory tracking with the PI control law. The initial posture of the mobile base was set as $(X_o,\ Y_o,\ \theta_o) = (30,\ 0,\ 0)$; the desired straight-line trajectory was set as

$$\left(X_d \quad Y_d \quad \theta_d\right) = \left(X_{do} + V_x t \quad Y_{do} + V_y t \quad \frac{\pi}{2}\right)$$

where $X_{do} = Y_{do} = 0,\ V_x = V_y = 3\ (cm/s)$. These results indicate that the proposed controller is capable of steering the mobile base to exponentially follow the desired line path.

6.3 Circular Trajectory Tracking

The experiment of the circular trajectory tracking was performed with the following parameters: $\omega_o = 0$ (rad/sec), $\omega_r = 0.3$ (rad/sec), $r = 20$ (cm), $Y_{do} = 0$, $X_{do} = 0$. The starting posture was given by $(X_o, Y_o, \theta_o) = (0,\ 0,\ 0)$, and the desired trajectory was described by

$$\left(X_d \quad Y_d \quad \theta_d\right) = \left(X_{do} + r \times \cos(\omega_o + \omega_r t) \quad Y_{do} + r \times \sin(\omega_o + \omega_r t) \quad \frac{\pi}{2}\right).$$

Fig. 10 presents the experimental result of the circular trajectory tracking for the omnidirectional mobile base with the PI control law. These results indicate that the kinematics controller has been shown useful in achieving the circular trajectory tracking.

6.4 Elliptic Trajectory Tracking

The last experiment was employed to explore how the PI controllers steer the mobile base to track an elliptic trajectory,

$$\left(X_d \quad Y_d \quad \theta_d\right) = \left(X_{do} + r_1 \times \cos(\omega_o + \omega_r t) \quad Y_{do} + r_2 \times \sin(\omega_o + \omega_r t) \quad \frac{\pi}{2}\right),$$

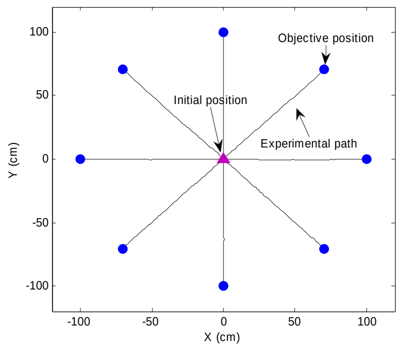

Fig. 8. Experimental results of the point-to-point kinematics control.

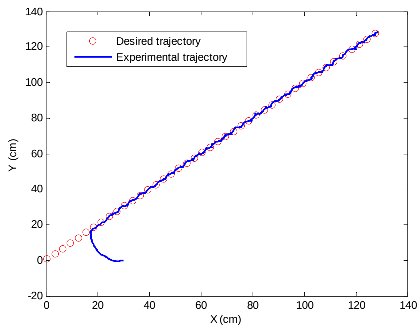

Fig. 9. Experiment result of the straight-line trajectory tracking.

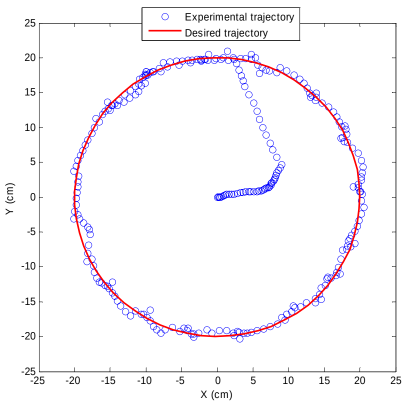

Fig. 10. Experimental result of the circular trajectory tracking.

and assumed that robots get started at zero initial posture, $(X_o, Y_o, \theta_o) = (0,\ 0,\ 0)$. The parameters in the elliptic trajectory tracking experiment were given as follows: $\omega_o = 0$ (rad/sec) , $\omega_r = 0.3$ (rad/sec) , $r_1 = 20$ (cm) , $r_2 = 30$ (cm) , $Y_{do} = 0$, $X_{do} = 0$. Fig. 11 depicts the elliptic trajectories of the omnidirectional mobile base. These results show that the kinematics controller is capable of steering the omnidirectional mobile robot to exactly move along with the elliptic trajectory.

7. Conclusions

This paper has developed methodologies for modeling and control of an omnidirectional mobile robot. With the kinematic diagram of the robot's

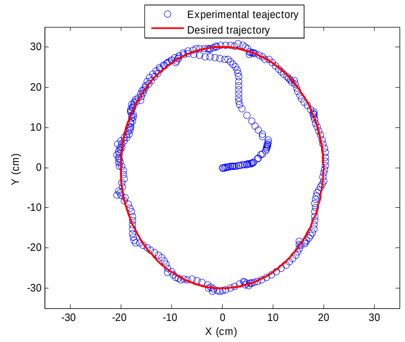

Fig. 11. Experimental result of the elliptic trajectory tracking.

wheels arrangement equally spaced at 120 degrees from one another, the kinematic model has been derived using the vector method. The kinematics PI controllers have been designed using feedback linearization to achieve point-to-point stabilization and trajectory tracking. Simulations and experimental results have shown that the kinematics PI controllers are capable of accomplishing desired regulation and trajectory tracking requirement. An important topic for future work will be to construct dynamic tracking controllers using low-cost digital signal processing to conduct several experiments in order to verify the proposed control methods incorporating with the actuator saturations and static friction.

REFERENCES

[1] F. G. Pin and S. M. Killough, “A new family of omnidirectional and holonomic wheeled platforms for mobile robots,” *IEEE Transaction on Robotics and Automation*, vol.10, no.4, pp.480-489, August 1994.

[2] M. J. Jung, H. S. Kim, S. Kim, and J. H. Kim, “Omni-directional mobile base OK-II,” *Proceeding of the 2000 IEEE international conference on Robotics and Automation*, San Franciso, CA, pp.3449-3454, April, 2000.

[3] T. Kalmar-Nagy, P. Ganguly, and R. D’andrea, “Real-time trajectory generation for omnidierectional vehicles,” *Proceedings of the American Control Conference*, Anchorage, AK, USA, pp. 286-291, 2002.

[4]R. L. Williams II, B. E. Carter, P. Gallina, and G. Rosati, “Dynamic model with slip for wheeled omnidirectional robots,” *IEEE Transaction on Robotics and Automation*, vol.18,no.3, pp.285293, June 2002.

[5] H. K. Khalil, *Nonlinear Systems*, 3rd Ed., Prentice Hall, 2002.

ACKNOWLEDGEMENTS

The authors gratefully acknowledge financial support from the National Science Council, Taiwan, R.O.C., under grant NSC 93-2213-E-005-038.